International Journal of Advanced Technology and Engineering Exploration, Vol 6(51)
ISSN (Print): 2394-5443 ISSN (Online): 2394-7454
http://dx.doi.org/10.19101/IJATEE.2019.650006

Research Article

Experimental and numerical analysis of a load distribution along the length of contact in involute spline shaft

Swapnil B. Patil[1*] and S. R. Patil[2]
ME Student, Department of Mechanical Engineering, AISSMS COE, SPPU, Pune, Maharashtra, India[1]
Assistant Professor, Department of Mechanical Engineering, AISSMS COE, SPPU, Pune, Maharashtra, India[2]

Received: 14-December-2018; Revised: 22-February-2019; Accepted: 25-February-2019

Abstract
In mechanical drive system for transmitting power the spline hub connections are widely used. Finite element method is used to find the load distribution along the length of spline, for analysis a frictional contact with 0.15 coefficient of friction and pure penalty method is used. For finding the load distribution three location is defined as entry, mid and exit. It is observed for partial spline contact over a length, two zones are created as contact and free zone. The analysis is performed for five partial contact length and torque respectively and it is observed that there is average 10.82% stress reduction at the entry point of spline and 64.60% stress reduction at the middle point of spline. There is no change is in the stress at the exit of a spline. The nature of the stresses in contact zone is uniformly decreasing toward the free zone and the stresses in free zone are also uniformly decreasing toward an exit of spline. The highly localized stress is identified in free zone probably at the end of percentage length of contact and this stresses uniformly decreasing toward the shoulder of spline shaft in the free zone. At the end of spline contact the stresses are high and this causes the failure of spline at this location.

Keywords
Involute spline shaft, Load distribution, Contact length, En19 alloy steel, Finite element analysis, Experimental stress analysis.

1.Introduction
The involute spline hub connection under pure torsion loading case aims to find the load distribution along the length of spline and localized stress area on teeth. Spline shaft for transmitting a torque is used. Properly align connection without sliding and angular misalignment is used. When the shaft is connected to a pure and study torque load, then the connection is under pure torsion loading condition. In pure torque transmitting case the spline teeth are under shear stress. In this paper the location for the stress along the spline length for partial contact length and the load distribution along the length of spline teeth is evaluated. Load distribution along the length of spline is measured by designing an experimental setup. The setup consists of spline connection mounted on the fixture. To apply a torque loading arm is used; strain gauges are installed on the teeth to measure the strain. The electronic system has facility to monitor the strains measured on the teeth.

*Author for correspondence

The study on the fix contact length for the spline hub connection is done in this paper. The study for the various contact length and load variation is done. The effect of change in contact length for the various torque cases is investigated. The experimental setup is designed with single channel strain indicator system which is helpful to determine the strain at the connection. For measuring a strain at the connection, the strain gauges with a compact size is used. The strain gauges mounted on the spline teeth along its length to predict the localized stress along the length. The spline shaft is designed with the En19 material characteristics and hub as well. Involute spline geometry is defined, as the involute spline geometry have a more load carrying capacity compared with the rectangular and traphizoidal spline geometry.

Experimental analysis in completed by using the strain gauge technique. The compact strain gauges are used along with the strain indicating device. The reading for strain value at entry, mid, exit portion of the spline length is taken and with the help of these strain stresses at that location is calculated from the

hooks law. The experiments are performed for the 50, 60, 70, 80, 90 mm spline contact with 86.6, 111.1, 135.63, 160.15, 184.68 Nm torque variations. The splines are tested under static pure torsion loading case by using the 15 to 35 kg with a load step of 5 kg.

The objectives of this paper are as follows:

1. To find the variation in load distribution along the length of spline contact for various contact length and torque levels combinations.
2. To predict the highly localized stress location along the length of spline contact.

2.Literature review

Hong et al. [1] Study the load distribution analysis of clearance-fit spline joints using finite elements and identified that load distribution along the spline length is different in case of spur and helical loading case. Pure torsion loading results showed identical load distributions on all spline teeth, with each tooth exhibiting non-uniform load in axial direction. Hong et al. [2] presented work on a semi analytical load distribution model for side-fit involute splines. The work aims to define semi analytical model to predict load distributions of spline joints. Adey et al. [3] developed an analysis tools for spline couplings. This study describes the development of new analysis technique to predict the contact stress and load transfer mechanism in spline coupling. Khalik and Faidh-Allah [4] studied experimental and numerical stress analysis of involute splined shaft. This induced splined shaft teeth contact and bending stresses have been investigated numerically using finite element method.

Tjernberg [5] presented work on the load distribution in axial direction in spline coupling; in this study the stress concentration factor at the teeth is considered. The stress concentration factor changes as the contact length changes. Barrot et al. [6] presented work on determined both radial pressure distribution and torsional stiffness of involute spline couplings. The analytical method is used to investigate the distortions of involute spline teeth. Barrot et al. [7] presented work on the extended equations of load distribution in the axial direction in a spline coupling to study of axial torque transfer in a spline coupling. The model developed by Tatur has been extended in order to consider different loading cases and geometries. AL-Shammaa and Kadhim [8] observed the effect of engagement length and spline parameters variation with cyclic crack growth rate in a spline coupling subjected to cyclic torsional impact have been investigated analytically and experimentally.

Ding et al. [9] work on finite element simulation of fretting wear fatigue interaction in spline couplings. This study describes a finite element based method for simulating the effects of material removal, associated with fretting wear, on fretting fatigue parameters in a spline coupling. Shen et al. [10] study plain fretting fatigue competition in spline shaft-hub connection. In this study the dynamically loaded spline shaft-hub connection that without macro relative movement between shaft and hub. Barsoum et al. [11] analyzed the torsional strength of hardened splined shafts. This study describe increasing the number of teeth, which corresponds to increasing the dedendum radius and keeping the addendum radius constant, increases the torsion strength of the shaft. Margineanu et al. [12] presented work on analytic and experimental study of the load distribution on spline joints length considering the contact rigidity of the bearing surfaces. In this study the load transfers by the spline under pure torsion condition.

Cuffaro et al. [13] identified the damage in spline coupling teeth by means of roughness parameters. The aim of this work is to use the surface roughness to identify the fretting damage on spline coupling teeth. Cura and Mura [14] presented a work on experimental procedure for the evaluation of tooth stiffness in spline coupling including angular misalignment. Tooth stiffness is a very important parameter in studying both static and dynamic behavior of spline couplings and gears. Xue et al. [15] modified the methodology of fretting wear in involute spline. This work gives the information about developing a method on predicting the fretting wear of spline couplings.

Qureshi et al. [16] investigates the principal component analysis for characterization of fretting wear experiments on spline couplings. Guo et al. [17] presented work on theoretical and experimental study on gear-coupling contact and loads considering misalignment, torque, and friction influences. A new analytic model addresses the tooth contact and induced loads of gear couplings that are affected by misalignment, torque, and friction. Pardhi and Khamankar [18] works on the stress analysis of spline shaft using finite element method and its experimental verification by photo elasticity. This research work deals with the stress in the spline shaft under various loading condition of given torque.

Finite element method along with experimental technique of photo elasticity is used.

3.Material properties and design parameters

External and internal splines are very extensively used in the automobile, machine tools and other industries.

The standard has been prepared to rationalize the production and to facilitate interchangeability of external and internal splines. The geometric characteristics of the internal and external spline are shown in *Figure 1*. The spline-hub design parameters are shown in the *Table 1*. The material properties for En19 material are given in *Table 2*

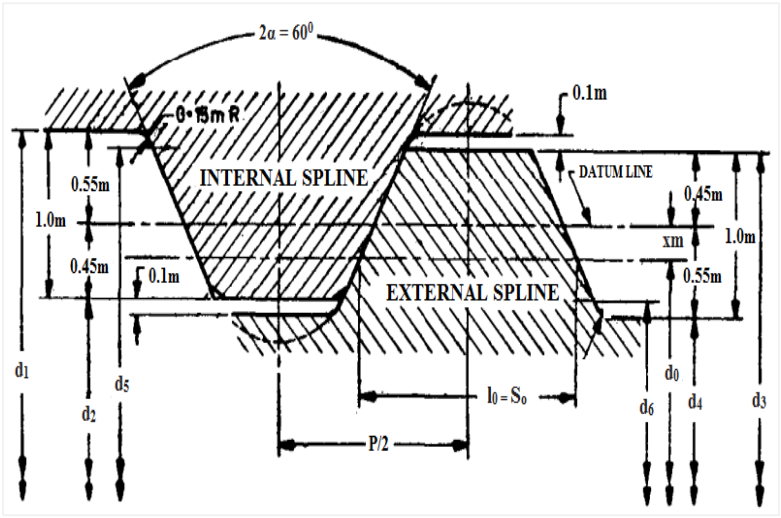

Figure 1 Profile characteristics of involute spline

Table 1 Design parameter for spline-hub connection

Sr.No.	Description	Symbol	Shaft	Hub
1	Module	m	4	4
2	No of teeth	z	10	10
3	Pressure angle	α	30^0	30^0
4	Addendum	h_a	1.80	1.80
5	Dedendum	h_d	2.2	2.20
6	Addendum modification	xm	1.30	1.30
7	Circular pitch	P	12.57	12.57
8	Tooth thickness	L_o	7.78	7.78
9	Pitch diameter	d_p	40	40
10	Base diameter	d_b	34.64	34.64
11	Major diameter	-	46.20	47
12	Minor diameter	-	38.20	39

Table 2 Material properties for En19 material

Sr.No.	Property	Parameter (MPA)
1	Young's modulus	204000
2	Poisson's ratio	0.3
3	Yield strength	816
4	Ultimate tensile strength	941

4.Finite element analysis

Finite element analysis for spline-hub connection is carried in ANSYS 14.5 for static pure torsion case. The spline shaft and hub is designed in CREO parametric 3.0 with En19 material properties.

CAD modeling

The 3D CAD model for spline contact is created in Creo 3.0; this parametric software gives good flexibility for modeling the involute spline profile. The solid part module is used to model a male and

female spline shaft, the involute spline profile is created by parametric curve generated through relation and parameters. The model contains an assembly of spline shaft and spline bush created in assembly model of Creo. The two contact bodies are created separately and assembled together to form a spline contact, now this model is then converted to STEP format to precede the finite element analysis. The 3D CAD model for spline shaft analysis is shown in *Figure 2*.

Define contact properties

Once material properties are given to coupling in ANSYS, contact elements need to define. Contact properties are given in four stages in ANSYS. In first stage contact class has to be defined. Generally, there are two contact classes: rigid-flexible and flexible-flexible. In rigid-flexible contact, one or more of the contacting surfaces are treated as rigid. The other class flexible-flexible contact is the more common type. In this case, all contacting bodies are deformable.

In second stage contact area has to be defined, there are two groups of contact point-surface contact and surface-surface contact. In ANSYS, the contact is generated by pair. For the point surface contact, the point is contact and the surface is target. For surface-surface contact, both contact and target are surfaces and they have to be specified which surface is contact and which is target. In model tree the contact option is there so the imported contact through model is need to delete because thus contact is not applicable, hence manual contact is defined. The contact and target body surfaces are shown in *Figure 3*.

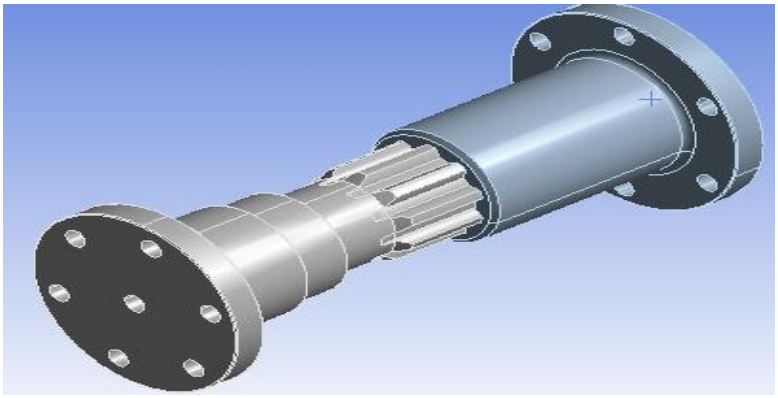

Figure 2 CAD model for FEA analysis

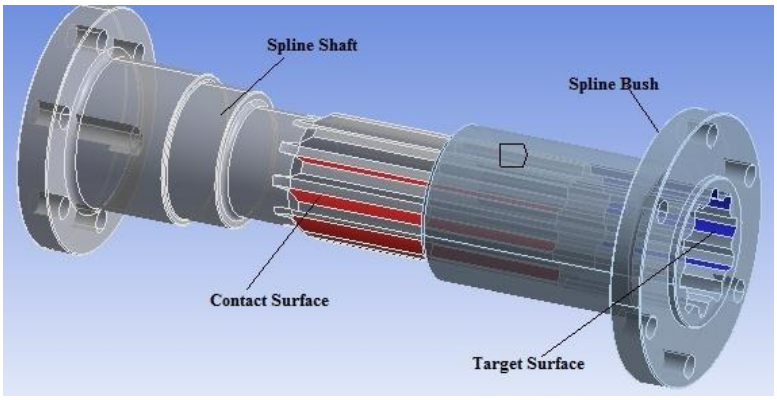

Figure 3 Contact preparations in FEA

In third stage behaviour of contact surface has to be specified. Contact surface has different types of behaviour according to different characteristics of contact. Normally there are frictional, no separation, bonded. In frictional contact, the contact body can slide on the target surface in the tangential direction. It can translate in the normal direction. This behaviour can simulate the contact opens and closes. Frictional contact is most reliable contact behaviour in analysis of spline hub connection. In bonded contact no relative movement between each other in

the rest of analysis is not possible. They look like one body. In this analysis we have used first frictional contact and after that bonded and no separation contact is used for checking best possible contact. In fourth stage contact algorithm has to be specified in ANSYS. Contact algorithms are used to solve contact problems. Normal Lagrange, pure penalty method and augmented Lagrange are three contact algorithm used to solve contact problems. In this analysis pure penalty method is used to solve contact problems.

Meshing

The contact preparation proceeds to the meshing of the model. The meshing is generated by programme control and the medium size of the element is selected. The programme evaluates the sizing characteristics and generates the mesh. The meshing model for the simulation is shown in *Figure 4*.

The spline-hub model meshed with tetrahedral element this element has better fitment over the area having sudden change in cross section. The tetrahedral element maintains the flow in the single direction. The size of the element is chosen to be medium size element programme control. The meshing characteristics for the spline-hub connection are given in *Table 3*.

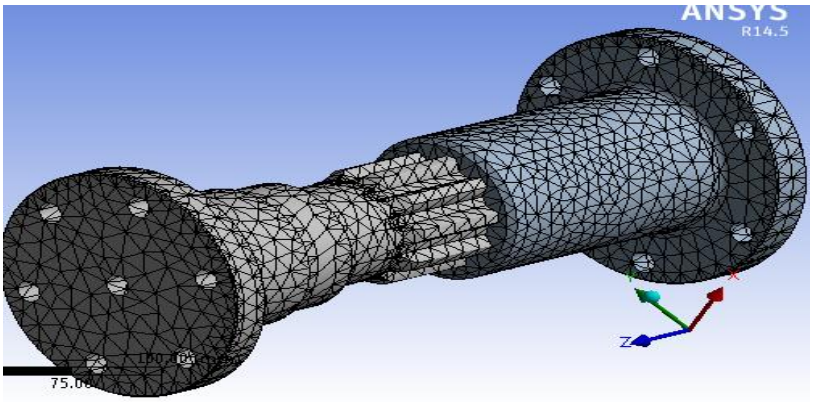

Figure 4 Meshing model of spline-hub connection

Table 3 Meshing characteristics for FEA

Sr. No.	Property	Parameter
1	Material	En19
2	Element type	Tetrahedral
3	Number of elements	33522
4	Number of nodes	58485

Set boundary conditions and apply loads

At this stage the boundary conditions are applied on the model to simulate with the practical situation. The spline bush flange is applied with fix support and spline shaft bearing locating surface is applied as frictionless surface and moment is applied on the spline shaft flange by using the components option. The spline bust is located on the load side always and hence it always generates a reaction torque on the spline contact to generate the reaction torque the bush is fixed and at the spline shaft end flange the toque is applied. A spline shaft is a driver component in the spline contact for power transmission. The spline hub connection is considered as a positive drive, the torque transmitted through is made possible without any power transmission loss. As the spline shaft is always at driver end the torque is always applied to the spline shaft. The boundary conditions are shown in *Figure 5*.

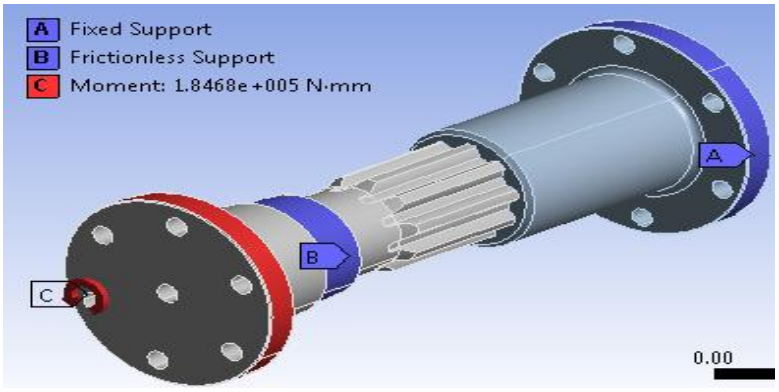

Figure 5 Boundary conditions and spline loading

The boundary conditions are applied on the spline hub connection, three parameters are used A defines the fixed support for the spline hub, B defines the frictionless support on the spline shaft where bearing is mounted, and C defines the torque flange on spline shaft.

5.Experimental stress analysis

For many materials within their elastic limit, there is a linear relationship between stress and strain. For uniaxial loading conditions, stress divided by strain is a constant known as Young's Modulus of Elasticity for the material. Thus, if strain can be measured, stress can be calculated. Strain is defined as the linear deformation of a material. It can occur as the result of the application of force or of temperature change. Unit strain e is the ratio of change in length divided by original length. This or dimensionless ratio is generally a very small decimal fraction, and is therefore usually multiplied by 10^{-6}, becoming "microstrain", με. The experimental setup for stress analysis is shown in *Figure 6*.

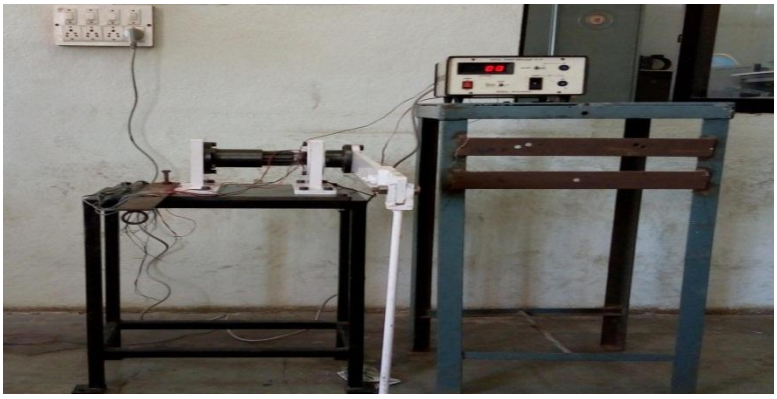

Figure 6 Experimental set for stress analysis

The static torque for the pure torsion loading is applied through the weight and arm arrangement for the case a torque values are calculated. The experimental stress analyses for spline-hub connection done by the strain gauge technique, compact strain gauges are used along with the strain indicating device.

The reading for strain value at entry, mid, exit portion of the spline length is taken with the help of strain gauges. The strain gauge location on spline shaft is shown in *Figure 7*. The stress at that location is calculated for the hooks law. The experiments are performed for the 50, 60, 70, 80, 90 mm spline contact with 86.6, 111.1, 135.63, 160.15, 184.68 Nm torque variations. The splines are tested under static pure torsion loading case by using the 15 to 35 kg with a load step of 5 kg.

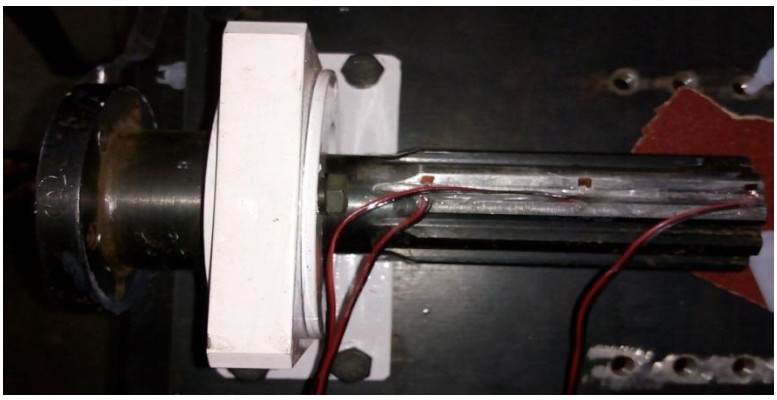

Figure 7 Strain gauges locations along the spline length

The experimentation is performed and the average percentage error for all contact length under study is calculated. The experimental analysis have some limitations to mount the strain gauges over the length of contact, for that the experimental and numerical validation is done at three locations at entry, mid and exit only. This validation gives the average percentage error for the reading taken, by using this percentage error we can calculate the remaining intermediate stresses for the other locations. The validation is performed for five different contact lengths. The total eleven stress readings along the length of spline are tabulated, to examine the nature of load distribution along the length of spline.

6.Results

The result of finite element analysis for frictional contact and pure penalty algorithm are observed. For frictional contact the coefficient of friction 0.15 is define. This methodology is used for 50, 60, 70, 80, 90 mm spline contact with 86.6, 111.1, 135.63, 160.15, 184.68 Nm torque. It is observed that the load distribution is similar in all spline. The equivalent elastic strain is shown in *Figure 8* and load distribution (Equivalent Von-Mises stresses) along the length of spline length in contact zone and free zone is shown in *Figure 9.*

When the splines are used for partial contact then the two zones are created one is free zone and another is a contact zone. The stresses at contact zone are less than the free zone. The stresses at the spline entry face are shown in the *Figure 10*. To identify the stress variation along the length of spline the three locations are decided entry middle and exit.

A data for the finite element analysis is observed, for load distribution along the length spline at multiple points along spline length. The stress variation along the length of spline is shown in *Figure 11*.

Figure 12 shows the shear stress distribution for 86.6 Nm torque along the percentage length of contact in 50, 60, 70, 80, 90 mm spline. It is observed that there is 9.13 % reduction in stress at the entry of spline and 64.80 % reduction is stress at the midpoint of spline contact.

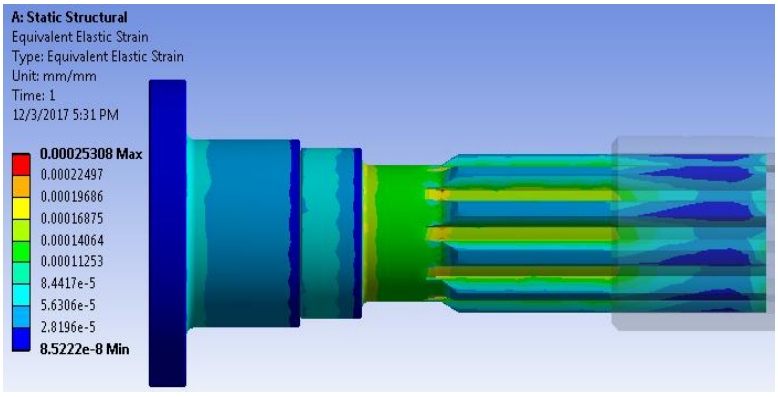

Figure 8 Variation in strain along the spline length

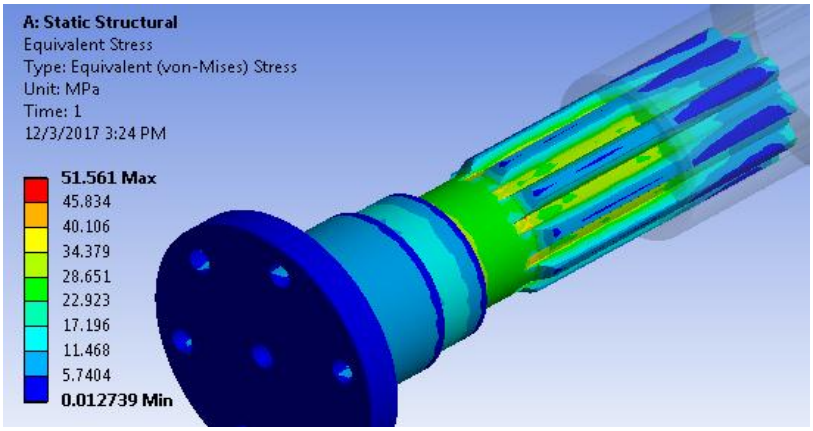

Figure 9 Stress variations along the spline length

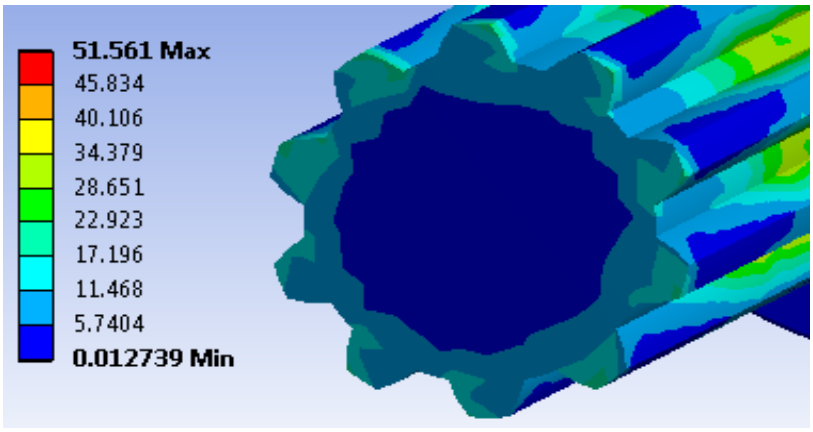

Figure 10 Stress variations at the entry of spline

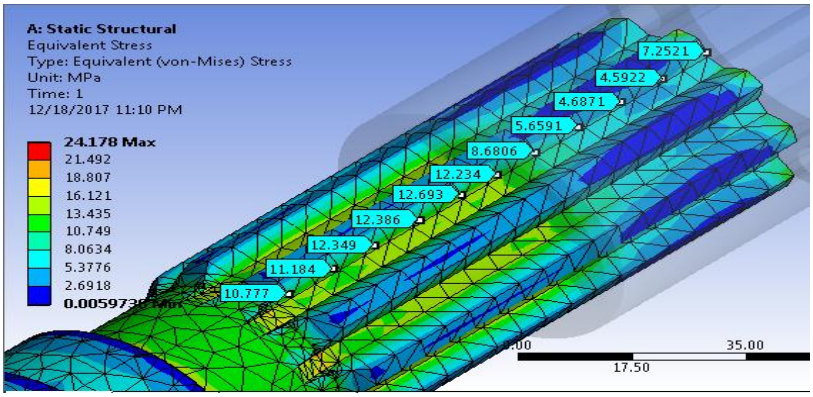

Figure 11 Stress variations along the length of spline

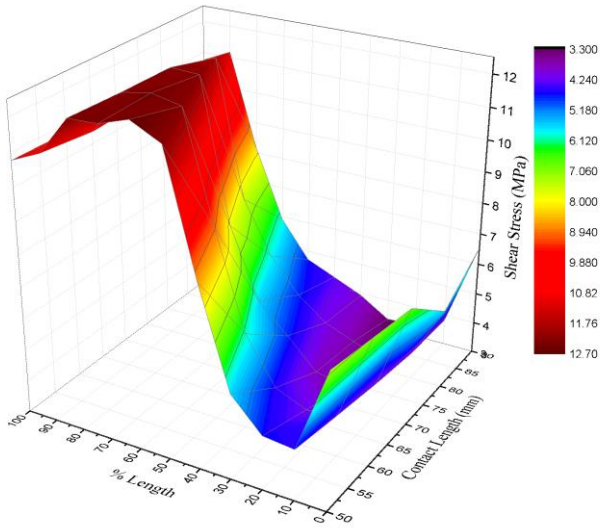

Figure 12 Shear stress distribution for 86.6 Nm torque

Figure 13 shows the shear stress distribution for 111.1 Nm torque along the percentage length of contact in 50, 60, 70, 80, 90 mm spline. It is observed that there is 10.10% reduction in stress at the entry of spline and 64.31 % reduction is stress at the midpoint of spline contact.

Figure 14 shows the shear stress distribution for 135.63 Nm torque along the percentage length of contact in 50, 60, 70, 80, 90 mm spline. It is observed that there is 11.18% reduction in stress at the entry of spline and 63.50 % reduction is stress at the midpoint of spline contact.

Figure 15 shows the shear stress distribution for 160.15 Nm torque along the percentage length of contact in 50, 60, 70, 80, 90 mm spline. It is observed that there is 11.79% reduction in stress at the entry of spline and 64.95 % reduction is stress at the midpoint of spline contact.

Figure 16 shows the shear stress distribution for 184.68 Nm torque along the percentage length of contact in 50, 60, 70, 80, 90 mm spline. It is observed that there is 11.90% reduction in stress at the entry of spline and 65.46% reduction is stress at the midpoint of spline contact.

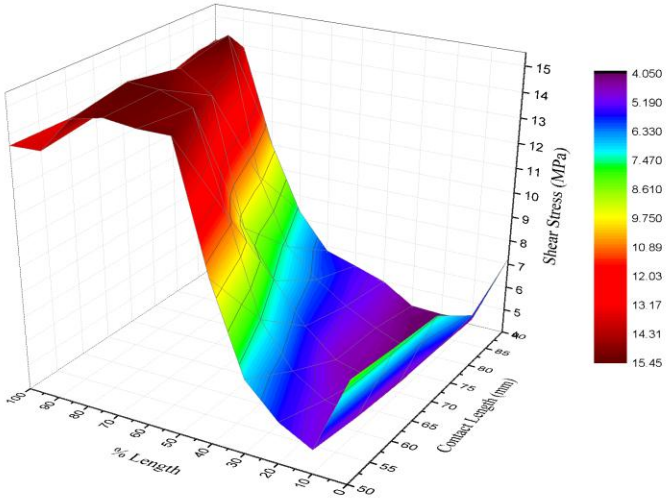

Figure 13 Shear stress distribution for 111.1 Nm torque

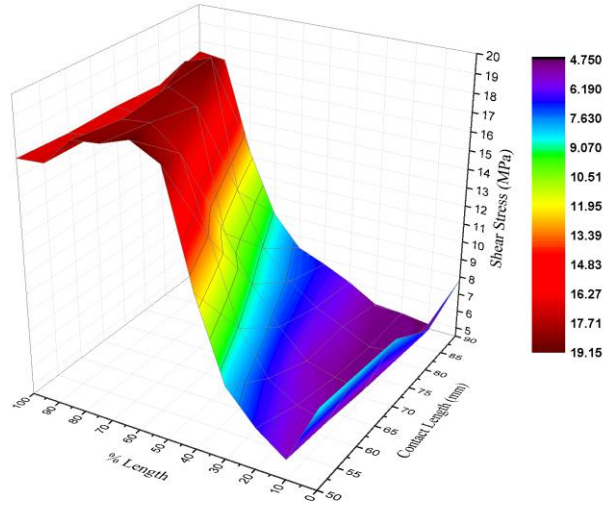

Figure 14 Shear stress distribution for 135.63 Nm torque

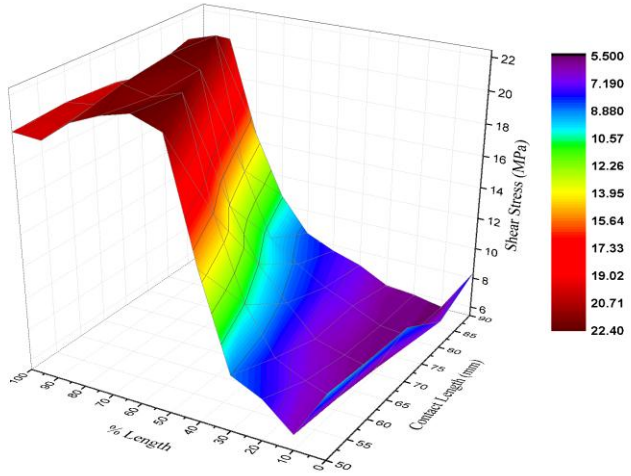

Figure 15 Shear stress distribution for 160.15 Nm torque

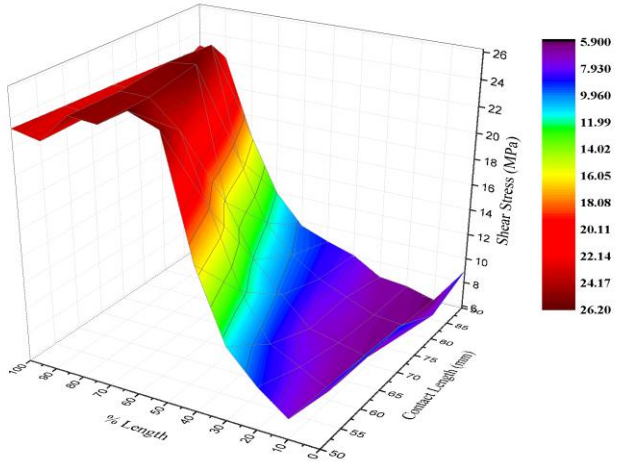

Figure 16 Shear stress distribution for 184.68 Nm torque

7.Discussion

The experimental stresses for the intermediate locations are calculated by using the percentage error application method. The percentage error for all cases under study is calculated from the experimental and finite element analysis performed for the 0, 50, 100% contact length. The comparison between the experimental and finite element analysis is done.

The average percentage error between experimental and finite element analysis for 86.6 Nm torque is 7.77%. The comparison between the experimental and finite element analysis for 86.6 Nm torque is shown in the *Figure 17*.

The average percentage error between experimental and finite element analysis for 111.1 Nm torque is 8.03%. The comparison between the experimental and finite element analysis for 111.1 Nm torque is shown in *Figure 18*.

The average percentage error between experimental and finite element analysis for 135.63 Nm torque is 7.50%. The comparison between the experimental and finite element analysis for 135.63 Nm torque is shown in *Figure 19*.

The average percentage error between experimental and finite element analysis for 160.15 Nm torque is 7.80%. The comparison between the experimental and finite element analysis for 160.15 Nm torque is shown in *Figure 20*.

The average percentage error between experimental and finite element analysis for 184.68 Nm torque is 7.65%. The comparison between the experimental and finite element analysis for 184.68 Nm torque is shown in *Figure 21*.

The comparison between the experimental and finite element analysis is observed and the nature of the stress variations along the length of contact is observed. Because of the partial length of contact the two zones are creating as contact and free zone. The nature of the stress variation curve is upstream within percentage length of contact (contact zone) and its starts changing its nature to downstream in the free zone.

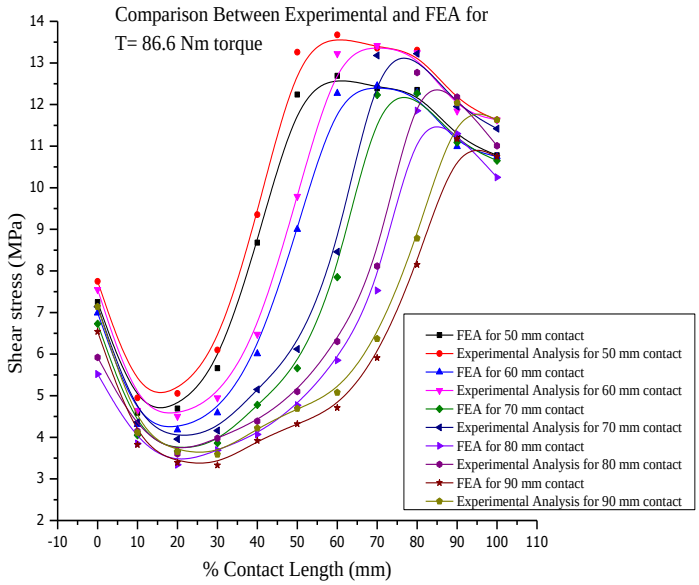

Figure 17 Comparison between experimental and FEA for 86.6 Nm torque

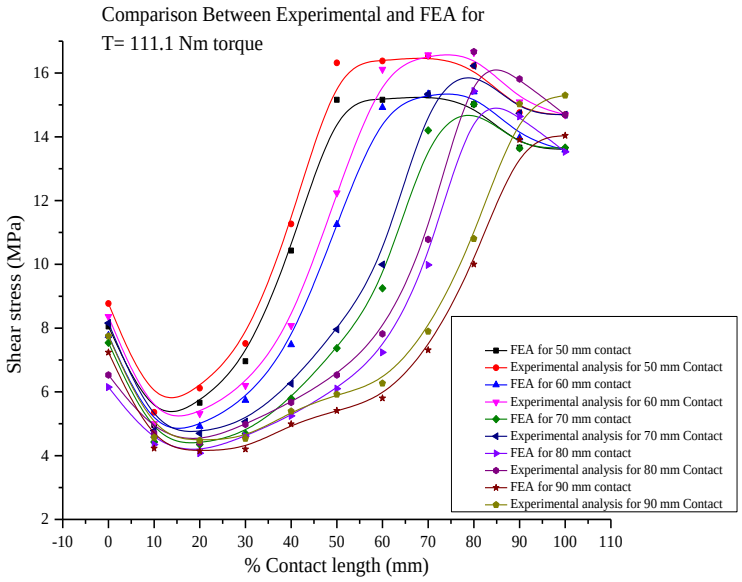

Figure 18 Comparison between experimental and FEA for 111.1 Nm torque

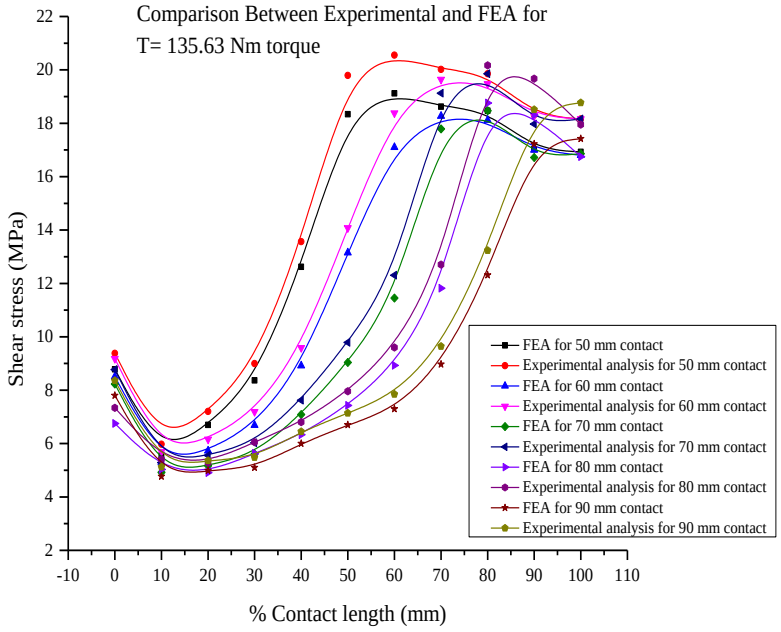

Figure 19 Comparison between experimental and FEA for 135.63 Nm torque

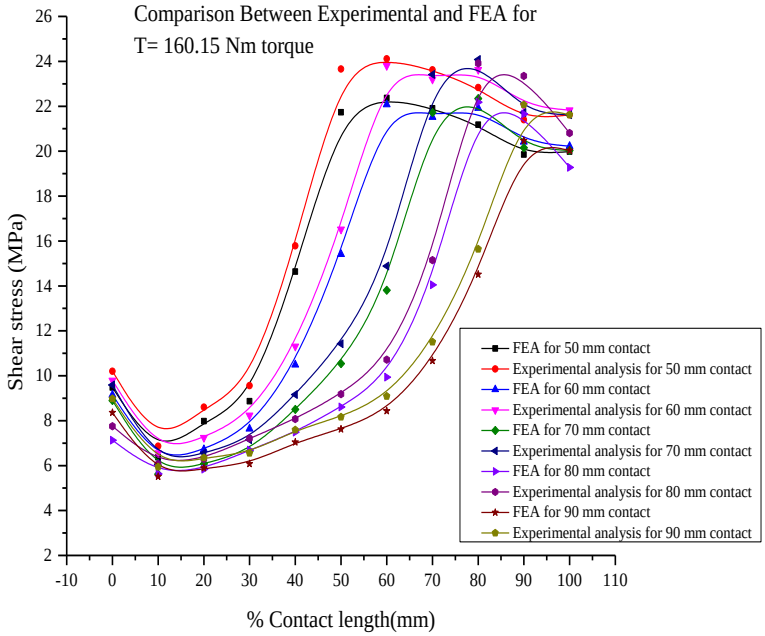

Figure 20 Comparison between experimental and FEA for 160.15 Nm torque

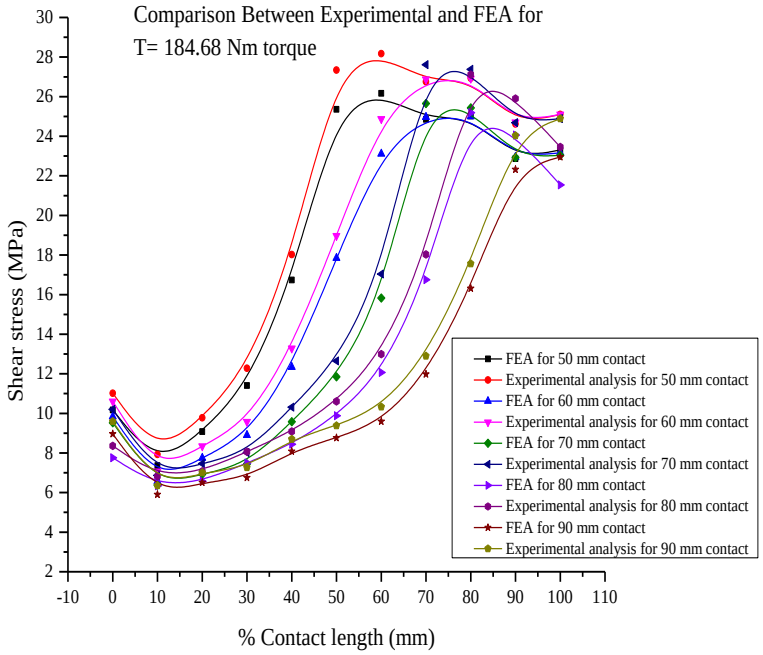

Figure 21 Comparison between experimental and FEA for 184.68 Nm torque

8.Conclusions and future scope

For finding the load distribution three location is defined as entry, mid and exit, and it is observed for partial spline contact over a length, two zones are created as contact zone and free zone.

The nature of the stresses in contact zone is uniformly decreasing toward the free zone. The stress at the contact zone is less as compare to free zone because at the contact zone the reaction force is generated by the hub pocket spline which neutral the effect of active shear force which results to less stress at contact zone.

The reaction force is not generating in free zone because of the partial spline contact length which results more stress at free zone as compare to contact zone.

It is predicted that there is 10.81% average stress reduction at the entry of spline. When the contact length is increases, contact zone also increases. It causes more spline profile area for shear stress distribution which leads to reduction in stress at the contact zone.

There is 64.60% average reduction is stress at the midpoint of spline. For contact more than 60 mm the midpoint lies in the contact zone, at midpoint the surface area available for shear force is more which leads to more percentage reduction in stress at this location.

The highly localized stress is identified in free zone probably at the end of percentage length of contact and this stresses uniformly decreasing toward the shoulder of spline shaft. There is negligible change observed at the exit of the spline for all analysis steps.

The nature of stress variation is same for all case taken under study and it is observed that the nature of curve for stress variation in contact zone is downstream and stress variation cure is upstream in free zone.

The stress at the end of contact is high because at the end of contact the spline profile is unsupported and experience a more torsion angle which leads to failure of spline at this location.

In future this work can be extended to find the load distribution in radial direction of spline, to find the load variations in radial direction an experimental set can be developed also the vibration analysis can be done in dynamic state for the different contact length of spline and load conditions.

Acknowledgment

None.

Conflicts of interest

The authors have no conflicts of interest to declare.

References

[1] Hong J, Talbot D, Kahraman A. Load distribution analysis of clearance-fit spline joints using finite elements. Mechanism and Machine Theory. 2014; 74:42-57.

[2] Hong J, Talbot D, Kahraman A. A semi-analytical load distribution model for side-fit involute splines. Mechanism and Machine Theory. 2014; 76:39-55.

[3] Adey RA, Baynham J, Taylor JW. Development of analysis tools for spline couplings. Proceedings of the Institution of Mechanical Engineers, Part G: Journal of Aerospace Engineering. 2000; 214(6):347-57.

[4] Khalik ZA, Faidh-Allah MH. Experimental and numerical stress analysis of involute splined shaft. Journal of Engineering. 2012; 18(4):415-22.

[5] Tjernberg A. Load distribution in the axial direction in a spline coupling. Engineering Failure Analysis. 2001; 8(6):557-70.

[6] Barrot A, Paredes M, Sartor M. Determining both radial pressure distribution and torsional stiffness of involute spline couplings. Proceedings of the Institution of Mechanical Engineers, Part C: Journal of Mechanical Engineering Science. 2006; 220(12):1727-38.

[7] Barrot A, Paredes M, Sartor M. Extended equations of load distribution in the axial direction in a spline coupling. Engineering Failure Analysis. 2009; 16(1):200-11.

[8] AL-Shammaa FA, Kadhim HF. An analysis of stress distribution in a spline shaft subjected to cycilc impulsive load. Journal of Engineering. 2014; 20(7):146-57.

[9] Ding J, Leen SB, Williams EJ, Shipway PH. Finite element simulation of fretting wear-fatigue interaction in spline couplings. Tribology-Materials, Surfaces & Interfaces. 2008; 2(1):10-24.

[10] Shen LJ, Lohrengel A, Schäfer G. Plain–fretting fatigue competition and prediction in spline shaft-hub connection. International Journal of Fatigue. 2013; 52:68-81.

[11] Barsoum I, Khan F, Barsoum Z. Analysis of the torsional strength of hardened splined shafts. Materials & Design (1980-2015). 2014; 54:130-6.

[12] Mărgineanu D, Mărgineanu E, Zăbavă ES, Fârtă AM. Analytic and experimental study of the load distribution on spline joints length considering the contact rigidity of the bearing surfaces. In Applied Mechanics and Materials 2012 (pp. 74-83). Trans Tech Publications.

[13] Cuffaro V, Curà F, Mura A. Damage identification on spline coupling teeth by means of roughness parameters. Theoretical and Applied Fracture Mechanics. 2016; 82:9-16.
[14] Cura F, Mura A. Experimental procedure for the evaluation of tooth stiffness in spline coupling including angular misalignment. Mechanical Systems and Signal Processing. 2013; 40(2):545-55.
[15] Xue X, Wang S, Li B. Modification methodology of fretting wear in involute spline. Wear. 2016; 368:435-44.
[16] Qureshi W, Cura F, Mura A. Principal component analysis for characterization of fretting wear experiments on spline couplings. Procedia Engineering. 2015; 109:73-9.
[17] Guo Y, Lambert S, Wallen R, Errichello R, Keller J. Theoretical and experimental study on gear-coupling contact and loads considering misalignment, torque, and friction influences. Mechanism and Machine Theory. 2016; 98:242-62.
[18] Pardhi DG, Khamankar SD. Stress analysis of spline shaft using finite element method and its experimental verification by photo elasticity. International Journal of Mechanical Engineering and Robotics Research. 2014; 3(4):451-8.

Mr. Swapnil B. Patil is currently pursuing his Masters of Engineering from AISSMS COE, Pune. He completed his B.E in Mechanical Engineering from JTM COE, Faizpur from North Maharashtra University, Jalgaon.

Email: patilswapnil091@gmail.com

Mr. S. R. Patil is currently working as Assistant Professor in AISSMS COE, Pune. He is pursuing his PhD in Mechanical Engineering in research area of NVH. He completed Masters of Engineering in Mechanical with specialization in Design Engineering and B.E. in Mechanical Engineering from Pune University.